

Prandtl-Number Dependence of Heat Transport in Laminar Horizontal Convection

Olga Shishkina* and Sebastian Wagner

Max Planck Institute for Dynamics and Self-Organization, Am Fassberg 17, D-37077 Göttingen, Germany

(Received 14 September 2015; published 15 January 2016)

We report the Prandtl-number (Pr) and Rayleigh-number (Ra) dependencies of the Reynolds number (Re) and mean convective heat transport, measured by the Nusselt number (Nu), in horizontal convection (HC) systems, where the heat supply and removal are provided exclusively through a lower horizontal surface of a fluid layer. For laminar HC, we find that $\text{Re} \sim \text{Ra}^{2/5} \text{Pr}^{-4/5}$, $\text{Nu} \sim \text{Ra}^{1/5} \text{Pr}^{1/10}$ with a transition to $\text{Re} \sim \text{Ra}^{1/2} \text{Pr}^{-1}$, $\text{Nu} \sim \text{Ra}^{1/4} \text{Pr}^0$ for large Pr. The results are based on direct numerical simulations for Ra from 3×10^8 to 5×10^{10} and Pr from 0.05 to 50 and are explained by applying the Grossmann-Lohse approach [J. Fluid Mech. 407, 27 (2000)] transferred from the case of Rayleigh-Bénard convection to the case of laminar HC.

DOI: 10.1103/PhysRevLett.116.024302

Horizontal convection (HC) [1–3] is a paradigm system to study heat and momentum transport in such flow configuration systems where heating and cooling are applied to different parts of the same horizontal surface of a fluid layer. This type of convection is relevant in many geophysical systems, in particular, in the large-scale ocean circulation [4], as heat is supplied to and removed from the ocean predominantly through its upper surface, where the ocean contacts the atmosphere [5]. HC is also relevant in process engineering; see, e.g., Ref. [6].

HC systems, in which the heat exchange takes place exclusively through the bottom plate, are determined mainly by the Rayleigh number $\text{Ra} \equiv \alpha g \Delta L^3 / (\kappa \nu)$, the Prandtl number $\text{Pr} \equiv \nu / \kappa$, and geometrical characteristics of the cell like the length-to-height aspect ratio $\Gamma = L/H$ and the relative areas of the heated and cooled surfaces compared to the bottom area. Here, ν denotes the kinematic viscosity, κ the thermal diffusivity, α the isobaric thermal expansion coefficient of the fluid, g the acceleration due to gravity, L the length, and H the height of the convection cell, and $\Delta \equiv (T_+ - T_-)$ with T_+ the temperature of the heated part of the bottom and T_- the temperature of the cooled part of the bottom.

The Rossby [5] model for the scaling with Ra and Pr of the mean heat flux, measured by the dimensionless Nusselt number $\text{Nu} \equiv -\langle \partial T / \partial z \rangle_+ / (\Delta / L)$, suggests $\text{Nu} \propto \text{Ra}^{1/5} \text{Pr}^0$, i.e., independence from Pr. Here, z is the vertical coordinate, T the temperature, and $\langle \cdot \rangle_+$ denotes the averaging over the heated part of the bottom and in time. The proportionality $\text{Nu} \propto \text{Ra}^{1/5}$ is supported by several numerical [6–10] and laboratory [1,9,11,12] experiments in nonturbulent HC, while the independence of Nu from Pr is not. For example, direct numerical simulations (DNS) by Gayen *et al.* [7] showed an increase of Nu with growing Pr, which is stronger for $\text{Pr} < 1$. The vertical-turbulent-plume model by Hughes *et al.* [11] suggests the scaling $\text{Nu} \propto \text{Ra}^{1/5} \text{Pr}^{1/5}$ with a Pr dependence, which, as we show

below, is too strong, at least for the here considered laminar HC flows.

In this Letter, we report DNS results on the dependences of the Reynolds number (Re) and Nu on Ra and Pr in laminar HC. The obtained results are in perfect agreement with the scaling power laws that one can derive by applying the Grossmann-Lohse [13] (GL) ansatz to the case of laminar HC. Namely, we exploit the idea that in laminar thermal convection, the time- and volume-averaged thermal and viscous dissipation rates are determined mainly by their boundary layer (BL) contributions. Note that the GL theory [13–17] for different scaling regimes in thermal convection was developed for the case of Rayleigh-Bénard convection (RBC) [18–22], in which the temperature T_+ is imposed at the whole bottom, the top temperature is set to T_- , and the reference distance L is the height of the cell.

In our DNS, we use the finite-volume code GOLDFISH to solve numerically the following equations in a Cartesian coordinate system $(x, y, z) \equiv (x_1, x_2, x_3)$, which describe HC flows in Boussinesq approximation: $\nabla \cdot \mathbf{u} = 0$ and

$$\partial \mathbf{u} / \partial t + \mathbf{u} \cdot \nabla \mathbf{u} + \rho^{-1} \nabla p = \nu \nabla^2 \mathbf{u} + \alpha g \theta \mathbf{e}_z, \quad (1)$$

$$\partial \theta / \partial t + \mathbf{u} \cdot \nabla \theta = \kappa \nabla^2 \theta, \quad (2)$$

with $\mathbf{u} \equiv (u_x, u_y, u_z)$ the velocity vector function, θ the reduced temperature, $\theta \equiv T - 0.5(T_+ + T_-)$, p the hydrodynamic pressure (without hydrostatic part), ρ the density, and $\mathbf{e}_z \equiv (0, 0, 1)^T$. On the domain boundaries, no-slip boundary conditions are considered: $\mathbf{u} = 0$. At the bottom heated part S_+ , holds $\theta = \Delta/2$, while $\theta = -\Delta/2$ on a cooled bottom part S_- . At the rest of the bottom and also at the top and side walls, $\partial \theta / \partial \mathbf{n} = 0$ holds with \mathbf{n} the unit normal vector.

The area $|S|$ of the bottom S and the area $|S_+|$ of the heated part of the bottom are related as $|S| = \Gamma |S_+|$, $\Gamma > 2$, and the areas of the heated and cooled parts are equal $|S_+| = |S_-|$. In our DNS, $\Gamma = 10$ is considered and the

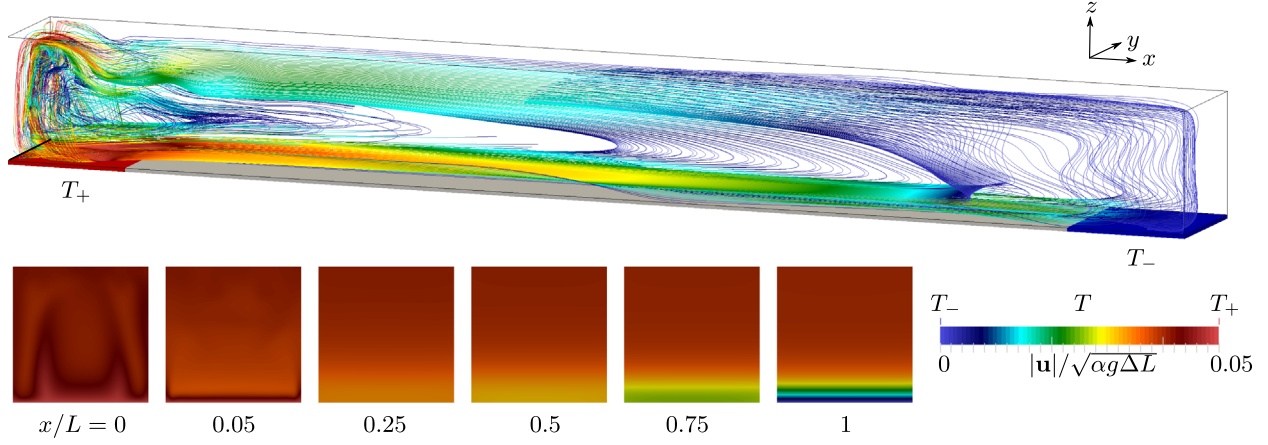


FIG. 1. Scheme of the studied HC setup together with the streamlines for $Ra = 10^{10}$ and $Pr = 1$, as obtained in the DNS. $1/10$ of the bottom is heated (left, $T = T_+$, red), while the other $1/10$ of the bottom is cooled (right, $T = T_- < T_+$, blue). The top and side walls and the rest of the bottom are adiabatic. Cross sections of the temperature snapshots are given below for $x = 0$, $x = 0.05L$ (at the center of the heated bottom part), $x = 0.25L$, $x = 0.5L$, $x = 0.75L$, and $x = L$.

length, height, and width of a parallelepiped computational domain are related as 10:1:1 (see a sketch of the studied HC setup in Fig. 1).

To investigate heat and momentum transport in laminar HC, we have conducted DNS for Ra from 3×10^8 to 5×10^{10} and Pr from 0.05 to 50 (see the details in Fig. 2). For lower Ra and not too small Pr , the HC flows are steady. With increasing Ra and decreasing Pr , the HC flows tend to be unsteady (see also, e.g., Ref. [7]). Therefore, to resolve the HC flows properly [23], we use different meshes in our simulations (see parameters of the computational meshes used in the DNS in the caption of Fig. 2). Note that HC flows are generally much slower and stabler than RBC flows for similar Rayleigh numbers. Thus, for $Pr = 1$ and $Ra = 10^9$, bulk flows in RBC are turbulent [24–27], while those in HC are still steady [7].

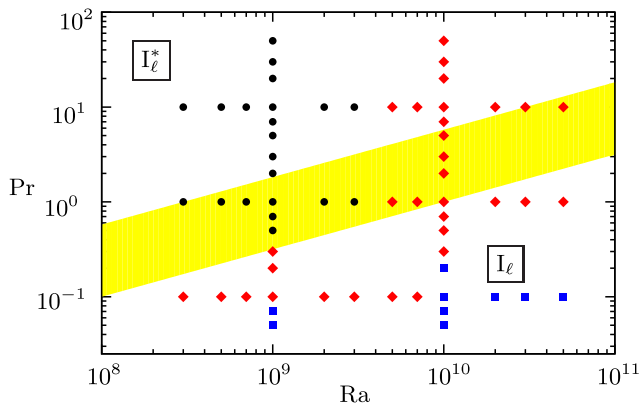


FIG. 2. Sketch of the phase diagram in the (Ra, Pr) plane for the laminar regimes I_ℓ and I_ℓ^* [28], together with the conducted DNS. The yellow stripe shows the transition from I_ℓ and I_ℓ^* , with a slope $Pr \sim Ra^{1/2}$. Symbols reflect the computational meshes in (x, y, z) , used in the DNS: $256 \times 32 \times 48$ (filled circle), $512 \times 64 \times 96$ (filled diamond), $1024 \times 90 \times 192$ (filled square).

The obtained results with respect to the scalings of Nu and Re with Ra and Pr in laminar HC are summarized in Fig. 3. For small and moderate Pr , the Nusselt number scales as $\sim Ra^{1/5}$ with a transition to $\sim Ra^{1/4}$ for large Pr [Fig. 3(a)]. For Re , which is evaluated as $(\overline{\mathbf{u} \cdot \mathbf{u}})^{1/2} L / \nu$, holds $Re \sim Ra^{2/5}$ [Fig. 3(c)]. Here, the bar denotes the time and volume average. For small Pr , the Pr dependence of the mean heat flux is $Nu \sim Pr^{1/10}$ [Fig. 3(b)], while for large Pr the Nusselt number is independent from Pr . Finally, the Reynolds number behaves as $Re \sim Pr^{-4/5}$ for smaller Pr and as $Re \sim Pr^{-1}$ for larger Pr [Fig. 3(d)].

The DNS results can be understood as follows. As laminar flows are considered here, the relation between Nu and $Re \equiv LU/\nu$, where U is the representative velocity of the large-scale flow (wind), can be obtained by balancing the terms in the thermal BL equation [13,19]

$$u_x \partial \theta / \partial x + u_z \partial \theta / \partial z = \kappa \partial^2 \theta / (\partial z)^2. \quad (3)$$

This yields $U\Delta/L \sim \kappa\Delta/\lambda_\theta^2$. Here, λ_θ is the (slope) thickness of the thermal BL, which scales as $\lambda_\theta \sim L/Nu$. The last two relations lead to

$$Nu \sim Re^{1/2} Pr^{1/2}. \quad (4)$$

The above relation between Nu , Re , and Pr is supported by our DNS results for laminar HC. In Figs. 4(a) and 4(b), the corresponding Ra and Pr dependences of $NuRe^{-1/2}$ are presented, which are in full agreement with (4).

In order to obtain the second scaling relation, in addition to (4), we follow the Grossmann and Lohse [13] approach for the case of laminar thermal convection. The balance of $\overline{\epsilon_u}$, which is the time- and volume-averaged kinetic dissipation rate $\epsilon_u \equiv \nu \sum_{i,j} (\partial u_j / \partial x_i)^2$, to its estimated BL contribution gives $\overline{\epsilon_u} \sim (\nu U^2 / \lambda_u^2) (\lambda_u / L)$, where λ_u is the thickness of the viscous BL near the bottom plate. This,

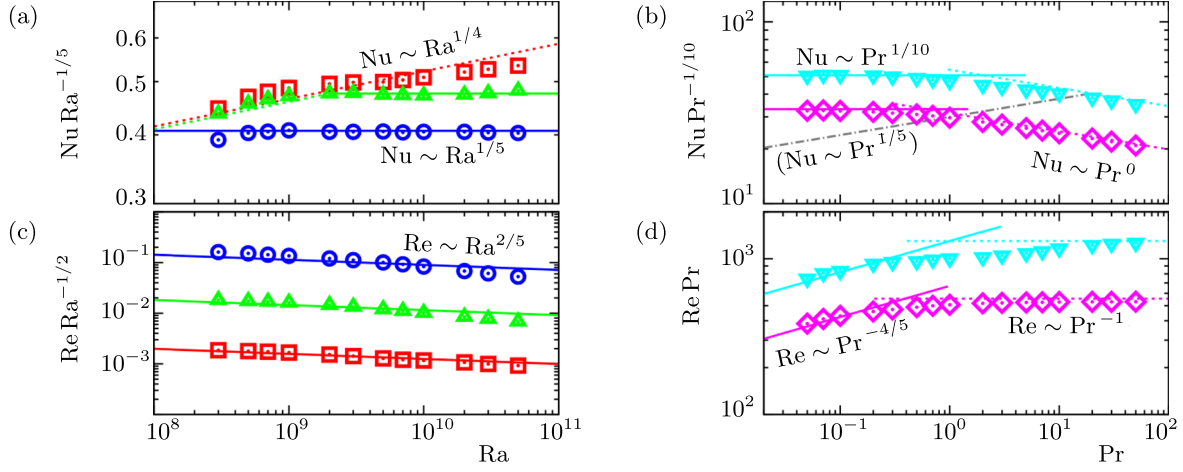


FIG. 3. (a),(c) Ra dependences and (b),(d) Pr dependences of (a),(b) the Nusselt number and (c),(d) the Reynolds number, as obtained in the DNS for (a),(c) $Pr = 0.1$ (dotted circle), $Pr = 1$ (upward triangle), $Pr = 10$ (dotted square) and for (b),(d) $Ra = 10^9$ (diamond) and $Ra = 10^{10}$ (downward triangle). The DNS results support the scalings in the regime I_ℓ (solid lines) [Eqs. (8) and (9)] and transition to I_ℓ^* (dotted lines) [Eqs. (11) and (12)]. In (b), the scaling $\sim Pr^{1/5}$ (dash-dotted line) is given for comparison and is not supported by the DNS.

together with $\lambda_u/L \sim Re^{-1/2}$ for laminar flows (see Sec. 39 in Ref. [29] and Ref. [30]), leads to

$$\overline{\epsilon}_u \sim (\nu^3/L^4) Re^{5/2}. \quad (5)$$

The time and volume average of (2) in combination with $\nabla \cdot \mathbf{u} = 0$ gives $\langle \partial\theta/\partial z \rangle_{z=0} = 0$, where $\langle \cdot \rangle_z$ denotes the

time and surface average at the height z . This, together with the average of (2) in time and over $S \times [0; z]$ for any $z \in [0; H]$, yields $\langle u_z \theta \rangle_z = \kappa \langle \partial\theta/\partial z \rangle_z$. Integration of this relation over $z \in [0; H]$ leads to

$$\overline{u_z \theta} = \kappa (\langle \theta \rangle_{z=H} - \langle \theta \rangle_{z=0}) / H = B(\Gamma - 1) \kappa \Delta / L, \quad (6)$$

where B is a certain constant $0 < B \leq 1$. Note that $B = 1$ only if $\langle \theta \rangle_{z=H} = \Delta/2$ and the temperature of the bottom between S_+ and S_- equals $(-\Delta/2)$. Multiplying (1) scalarly by \mathbf{u} and further integrating in time and over the domain and taking into account (6), we obtain

$$\begin{aligned} \overline{\epsilon}_u &= \alpha g \overline{u_z \theta} = B(\Gamma - 1) \alpha g \kappa \Delta L^{-1} \\ &= \nu^3 L^{-4} B(\Gamma - 1) Ra Pr^{-2}. \end{aligned} \quad (7)$$

The above relation is also fully supported by our numerical results, presented in Figs. 4(c) and 4(d). As $(L^4/\nu^3) \overline{\epsilon}_u Ra^{-1}$ is independent from Ra [Fig. 4(c)] and depends on Pr as $\sim Pr^{-2}$ [Fig. 4(d)], from this we conclude that the factor B in (7) is a constant, which is independent from Ra and Pr and can depend only on the cell geometry. For the considered HC setup, our DNS show that the value of $B(\Gamma - 1)$ is about 2.

Thus, from (4), (5), and (7), one obtains the scalings in the laminar regime in HC:

$$Re \sim Ra^{2/5} Pr^{-4/5}, \quad (8)$$

$$Nu \sim Ra^{1/5} Pr^{1/10}. \quad (9)$$

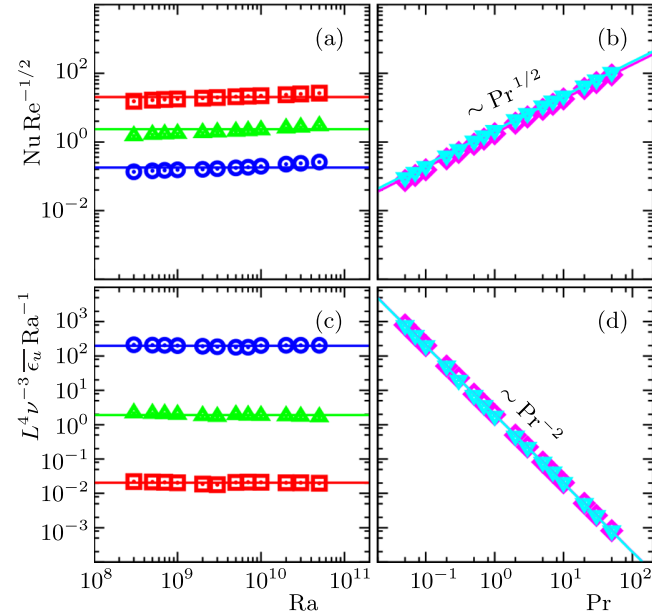


FIG. 4. (a),(c) Ra dependences and (b),(d) Pr dependences of (a),(b) $Nu Re^{-1/2}$ and (c),(d) $(L^4/\nu^3) \overline{\epsilon}_u Ra^{-1}$, as obtained in the DNS for (a),(c) $Pr = 0.1$ (dotted circle), $Pr = 1$ (upward triangle), $Pr = 10$ (dotted square) and for (b),(d) $Ra = 10^9$ (diamond) and $Ra = 10^{10}$ (downward triangle). The upper figures support (4), while the lower figures illustrate the correctness of the estimate (7).

By analogy to the notation in the Grossmann-Lohse theory for RBC [13], this scaling regime is denoted as I_ℓ , where the subscript ℓ stands for low-Pr fluids.

With decreasing Ra, the BL thickness λ_u generally increases. Because of the geometrical restrictions, the growth of the BL thickness is limited and λ_u saturates to a certain bounded value. In this case, the BL contribution to the mean kinetic dissipation rate scales as $\bar{\epsilon}_u \sim (\nu U^2/L^2)$, which yields

$$\bar{\epsilon}_u \sim (\nu^3/L^4)\text{Re}^2. \quad (10)$$

From (4), (7), and (10), it follows that

$$\text{Re} \sim \text{Ra}^{1/2} \text{Pr}^{-1}, \quad (11)$$

$$\text{Nu} \sim \text{Ra}^{1/4} \text{Pr}^0 \quad (12)$$

in that particular region of the (Ra, Pr) plane. This scaling regime is denoted as I_ℓ^* in Fig. 2.

The slope of the transition region in the (Ra, Pr) plane, between the laminar regimes I_ℓ and I_ℓ^* , is determined by matching the Nusselt numbers in these neighbor regimes. Thus, from Eqs. (9) and (12), we obtain the slope of the transition region between the regimes I_ℓ and I_ℓ^* , which is $\text{Pr} \sim \text{Ra}^{1/2}$. The location of the transition region is highlighted by a stripe in the (Ra, Pr) plane in Fig. 2 and is estimated from the DNS data, by considering the changes in the Nu(Ra, Pr) and Re(Ra, Pr) dependences. Note that the transition is smooth and can be affected by the geometry of particular HC setups.

To conclude, we studied in the DNS laminar HC and found that $\text{Re} \sim \text{Ra}^{2/5} \text{Pr}^{-4/5}$, $\text{Nu} \sim \text{Ra}^{1/5} \text{Pr}^{1/10}$ with a transition to $\text{Re} \sim \text{Ra}^{1/2} \text{Pr}^{-1}$, $\text{Nu} \sim \text{Ra}^{1/4} \text{Pr}^0$ for large Pr. Investigations of further anticipated scaling regimes for unsteady and turbulent HC flows [28] are beyond the scope of this Letter and are the subject of forthcoming experimental and numerical studies.

The authors would like to thank Eberhard Bodenschatz, Siegfried Grossmann, and Detlef Lohse for fruitful discussions and their support of this study. The authors acknowledge also financial support of the Deutsche Forschungsgemeinschaft (DFG) under Grants No. Sh405/3 and No. Sh405/4 (Heisenberg fellowship) and Leibniz Supercomputing Centre (LRZ) for providing computing time.

*Olga.Shishkina@ds.mpg.de

- [1] R. W. Griffiths, G. O. Hughes, and B. Gayen, *J. Fluid Mech.* **726**, 559 (2013).
 [2] G. O. Hughes and R. W. Griffiths, *Annu. Rev. Fluid Mech.* **40**, 185 (2008).

- [3] M. E. Stern, *Ocean Circulation Physics* (Academic, New York, 1975).
 [4] B. Cushman-Roisin and J.-M. Beckers, *Introduction to Geophysical Fluid Dynamics. Physical and Numerical Aspects*, 2nd ed. (Academic, New York, 2011).
 [5] H. T. Rossby, *Deep-Sea Res.* **12**, 9 (1965).
 [6] S. Chiu-Webster, E. J. Hinch, and J. R. Liter, *J. Fluid Mech.* **611**, 395 (2008).
 [7] B. Gayen, R. W. Griffiths, and G. O. Hughes, *J. Fluid Mech.* **751**, 698 (2014).
 [8] B. Gayen, R. W. Griffiths, G. O. Hughes, and J. A. Saenz, *J. Fluid Mech.* **716**, R10 (2013).
 [9] J. C. Mullarney, R. W. Griffiths, and G. O. Hughes, *J. Fluid Mech.* **516**, 181 (2004).
 [10] H. T. Rossby, *Tellus* **50**, 242 (1998).
 [11] G. O. Hughes, R. W. Griffiths, J. C. Mullarney, and W. H. Peterson, *J. Fluid Mech.* **581**, 251 (2007).
 [12] W. Wang and R. X. Huang, *J. Fluid Mech.* **540**, 49 (2005).
 [13] S. Grossmann and D. Lohse, *J. Fluid Mech.* **407**, 27 (2000).
 [14] S. Grossmann and D. Lohse, *Phys. Rev. Lett.* **86**, 3316 (2001).
 [15] S. Grossmann and D. Lohse, *J. Fluid Mech.* **486**, 105 (2003).
 [16] S. Grossmann and D. Lohse, *Phys. Fluids* **16**, 4462 (2004).
 [17] S. Grossmann and D. Lohse, *Phys. Fluids* **23**, 045108 (2011).
 [18] B. Castaing, G. Gunaratne, F. Heslot, L. Kadanoff, A. Libchaber, S. Thomae, X.-Z. Wu, S. Zaleski, and G. Zanetti, *J. Fluid Mech.* **204**, 1 (1989).
 [19] E. Siggia, *Annu. Rev. Fluid Mech.* **26**, 137 (1994).
 [20] G. Ahlers, S. Grossmann, and D. Lohse, *Rev. Mod. Phys.* **81**, 503 (2009).
 [21] F. Chillà and J. Schumacher, *Eur. Phys. J. E* **35**, 58 (2012).
 [22] O. Shishkina, S. Horn, S. Wagner, and E. S. C. Ching, *Phys. Rev. Lett.* **114**, 114302 (2015).
 [23] O. Shishkina, R. J. A. M. Stevens, S. Grossmann, and D. Lohse, *New J. Phys.* **12**, 075022 (2010).
 [24] O. Shishkina, S. Wagner, and S. Horn, *Phys. Rev. E* **89**, 033014 (2014).
 [25] S. Wagner and O. Shishkina, *Phys. Fluids* **25**, 085110 (2013).
 [26] X. He, E. S. C. Ching, and P. Tong, *Phys. Fluids* **23**, 025106 (2011).
 [27] M. Kaczorowski, O. Shishkina, A. Shishkin, C. Wagner, and K.-Q. Xia, in *Direct and Large-Eddy Simulation VIII*, edited by H. Kuerten, B. Geurts, V. Armenio, and J. Fröhlich (Springer, New York, 2011), p. 383.
 [28] O. Shishkina, S. Grossmann, and D. Lohse (to be published).
 [29] L. D. Landau and E. M. Lifshitz, *Fluid Mechanics*, Vol. 6, Course of Theoretical Physics, 2nd ed. (Butterworth-Heinemann, Oxford, 1987).
 [30] O. Shishkina, S. Horn, and S. Wagner, *J. Fluid Mech.* **730**, 442 (2013).